The phosphorylation site in double helical amylopectin as investigated by a combined approach using chemical synthesis, crystallography and molecular modeling

Søren Balling Engelsen[a,*], Anders Østergaard Madsen[b], Andreas Blennow[c],
Mohammed Saddik Motawia[c], Birger Lindberg Møller[c], Sine Larsen[b]

[a] Food Technology, Department of Dairy and Food Science, The Royal Veterinary and Agricultural University, Rolighedsvej 30,
DK-1958 Frederiksberg C, Denmark
[b] Centre for Crystallographic Studies, Department of Chemistry, University of Copenhagen, Universitetsparken 5, DK-2100 Copenhagen Ø, Denmark
[c] Plant Biochemistry Laboratory, Center for Molecular Plant Physiology (PlaCe), Department of Plant Biology,
The Royal Veterinary and Agricultural University, Thorvaldsensvej 40, DK-1871 Frederiksberg C, Denmark

Abstract The only known in planta substitution of starch is phosphorylation. Whereas the function of starch phosphorylation is poorly understood, phosphorylated starch possesses improved functionality in vitro. Molecular models of native crystalline starch are currently being developed and the starch phosphorylating enzyme has recently been discovered. Accordingly, it is desirable to obtain a more exact description of the molecular structures of phosphorylated starch. We have determined the crystal structure of methyl α-D-glucopyranoside 6-O-phosphate as its potassium salt which is thought to be the starch phosphate counterion in vivo. From this structure and previously known glucophosphate structures we describe the possible 6-O-phosphate geometries and through modeling extrapolate the results to the double helical structure of the crystalline part of amylopectin. The geometries of the existing crystal structures of 6-O-phosphate groups were found to belong to two main adiabatic valleys. One of these conformations could be fitted into the double helical amylopectin part without perturbing the double helical amylopectin structure and without creating steric problems for the hexagonal chain–chain packing.

1. Introduction

Starch is deposited in plastids as granules ranging 1–100 μm in diameter. The main components of the granules are amylopectin and amylose, both homopolymers of glucose. Amylopectin is composed of α-1,4-linked glucose units of which approximately 5% carry side chains attached by an α-1,6-glucosidic linkage. Amylopectin also contains varying amounts of mono-esterified phosphate groups. Amylose, which constitutes approximately 20–30% of the granule mass in normal storage starches is essentially unbranched, it does not contain significant amounts of covalently linked phosphate nor does it

normally contribute to the overall starch granule crystallinity or morphology.

A unique feature of the starch granule is the arrangement of amylopectin α-glucan chains in highly organized liquid crystalline lamellar super-helical structures [1,2]. Powder X-ray crystallography has revealed that native starch granules crystallize in two principal different ways – the A-type or B-type crystalline polymorph. A constant 9–10 nm radial ordered repeat in starch granules has been demonstrated by small angle X-ray scattering experiments [3] and electron microscopy [1]. Based on fiber X-ray diffraction crystallography studies and molecular models more precise structures of the A- [4] and B-type [5] polymorphs have been generated [6]. Both correspond to parallel, left-handed double helices with 2.1 nm pitch height and six glucose units per turn. The helical conformations are very similar for the A- and B-type polymorphs. Recently, a force-field modeling approach included the inter-helix branch point and the single chain inter-helix spacer length parameters in the helix-packing model [7].

Starches of different plant origin, especially those from tuberous tissues, contain phosphate groups mono-esterified to the glucose residues. In the highest substituted potato starches reported, one out of 200 glucose residues is substituted [8,9]. The most highly substituted natural starch currently known has a degree of substitution of 1% [8,10,11]. The phosphate groups are linked to the C-3 and C-6 positions of the glucose residues [9,12]. Long unit chains are more highly substituted than short ones [13–15] and C-6 phosphate substitution is more pronounced in amorphous regions [8]. The covalently bound phosphate increases hydration of starch pastes and hence, the starch phosphate content affects, for example, the starch paste peak viscosity [16–18].

The molecular events taking place during starch synthesis and deposition are poorly understood. Synthesis of amylopectin is achieved by a concerted action of isoforms of starch-synthesizing enzymes which have different substrate specificities [19]. Starch phosphorylation is an integral part of starch biosynthesis [20]. The reaction mechanism of a starch phosphorylating enzyme, called R1 [21], was recently resolved and shown to involve phosphoryl transfer by a dikinase-type reaction where the β-phosphate of adenosine triphosphate (ATP) was transferred to both the C-6 and C-3 positions of

*Corresponding author. Fax: (45)-35-28 32 45.
E-mail address: se@kvl.dk (S.B. Engelsen).

the glucose residues in starch and the γ-phosphate was transferred to water [22]. Hence, the starch phosphorylating enzyme is an α-glucan water dikinase (GWD). Mutants of *Arabidopsis thaliana* in which the GWD has been knocked out [23] and transgenic potato plants with suppressed GWD [21] show, in addition to suppressed starch phosphorylation, a starch excess phenotype suggesting a direct relationship between starch phosphorylation and degradation. The biochemical basis for this link remains elusive, but starch phosphorylation is now considered a crucial and integrated part of starch metabolism [24]. Manipulation of enzymes directly involved in the build-up of amylopectin is known to affect the chain length distribution of the amylopectin side chains and the level of starch-bound phosphate. Antisense suppression of the total soluble starch synthase (SS) activity in potato depresses the starch phosphate content [25]. However, suppression of the SS III isoform increases the phosphate content by 70% [26]. Likewise, an increase of the average amylopectin chain length by suppression of the total starch branching enzyme (SBE) activity dramatically increases the content of phosphate groups [10]. In general, the natural variation in starch phosphorylation is observed to be positively correlated to the average chain length of the amylopectin side chains [15]. In particular, a population of chains with a degree of polymerization (DP) of approximately 20 seems important, as confirmed by chain length profiles of starches prepared from tubers of transgenic potato lines with suppressed SBE activity [10].

To improve our current knowledge of the in vivo importance of starch phosphorylation, the present study was undertaken to obtain molecular details of the phosphorylation site in double helical amylopectin. For this purpose we have synthesized a methyl α-D-glucopyranoside 6-*O*-phosphate as a first model structure of amylopectin phosphorylation. The methyl glucoside was chosen in order to mimic an elongation of the glucoside backbone [27] and to prevent mutarotation. The new compound was investigated by X-ray analysis and compared to existing structures of glucose 6-*O*-phosphates and the results extrapolated to a possible phosphorylation site in double helical amylopectin. The phosphorylation site in amylopectin is evaluated by X-ray evidence, mass spectrometry and molecular modeling.

2. Materials and methods

2.1. Chemical synthesis of methyl α-D-glucopyranoside 6-O-phosphate

Treatment of commercially available methyl α-D-glucopyranoside with *tert*-butyldiphenylsilyl chloride in DMF containing imidazole [28] and purification on silica gel column chromatography furnished the corresponding 6-*O*-*tert*-BDPSi derivative in 80% yield. Benzylation of the 6-*O*-*tert*-BDPSi derivative with benzyl bromide under phase-transfer catalysis conditions using tetrabutylammonium hydrogen sulfate (TBAHS) [29,30] provided the tri-*O*-benzylated derivative in 85% yield after chromatographic purification. Removal of the *tert*-BDPSi group was accomplished using tetrabutylammonium fluoride (TBAF) in THF [28] to regenerate the parent alcohol [31] in 93% yield. Phosphorylation with diphenyl chlorophosphate in dichloromethane containing *N,N*-dimethylaminopyridene (DMAP) afforded the 6-*O*-diphenyl phosphate derivative in 92% yield after purification on silica gel column chromatography. Stepwise catalytic hydrogenolysis to remove the benzyl-protecting groups using 20% palladium hydroxide-*on*-charcoal under atmospheric hydrogen and subsequent use of Adam's catalyst under hydrogen atmosphere to remove the phenyl-protecting groups provided methyl-D-glucopyranoside 6-*O*-phosphate (Fig. 1) which was purified as previously described [32]

Table 1
Crystal data and structure determination data

Crystal data and structure refinement for methyl α-D-glucopyranoside 6-*O*-phosphate	
Empirical formula	$C_7H_{14}KO_9P$
Formula weight	312.25 g/mol
Temperature	122.0(5) K
Wavelength	1.54180 Å
Crystal system, space group	orthorhombic, $P2_12_12_1$
Unit cell dimensions	$a = 20.267(2)$ Å
	$b = 4.9108(5)$ Å
	$c = 11.8091(5)$ Å
Volume	1175.3(3) Å^3
Z	4
Calculated density	1.765 Mg/m^3

and converted into the desired potassium salt. The nuclear magnetic resonance (NMR) spectral data were in agreement with the reported data for the disodium salt [32].

2.2. Crystallization

The potassium salt of methyl glucose 6-phosphate was prepared by passing the acid form over a K^+ Dowex 50 W column and subsequently lyophilized. The precipitated potassium saccharide (3 mg) was dissolved in 1 ml of 70% 2-propanol, 30% water adjusted to pH 3.5 with HCl. Aliquots (50 μl) were applied in MVD/24 crystal growth chambers (Charles Supper Company, Natick, MA, USA) and equilibrated by vapor diffusion against 80% 2-propanol, pH 3.5 at 28°C for 7 days. Crystals (plates) were repeatedly seeded three times in order to achieve sufficient thickness.

2.3. Crystal structure determination

Low temperature X-ray diffraction data (122.4(1) K) were collected on an Enraf Nonius CAD4 diffractometer using graphite monochromated Cu K_α radiation. The data were corrected for background, Lorentz and polarization effects, and an absorption correction by numerical integration applied using the DREADD programs [33]. The structure (Fig. 1), crystallizing in the orthorhombic space group $P2_12_12_1$, was determined and refined using the SHELX program package [34]. All hydrogen atoms were located from difference maps and refined freely with isotropic displacement parameters. The final refinement statistics were $R_w^2 = 0.055$, Goof = 4.3 and −0.003(8) for the Flack parameter. This indicates that the structure as well as the absolute configuration are well determined. See Table 1 for crystal and data collection data. Coordinates have been deposited in the Cambridge Structural Data Centre[1].

2.4. Mass spectrometry

Mass spectra of potato starch samples were recorded using a HP G2025A matrix-assisted laser desorption/ionization time-of-flight (MALDI-TOF) mass spectrometer (Hewlett-Packard, Palo Alto, CA, USA). A probe with 10 mesa was used and 1 ml of starch-matrix solution was applied to each mesa. The range was up to 10 000 Da, in a linear positive mode with an acceleration voltage of 28 kV and a sampling rate of 200 MHz. Ions were formed using a pulsed nitrogen laser with pulse width at 3 ns operating at 337 nm. All spectra were recorded at a tube pressure below 9×10^{-6} Torr. The flight tube was 1.0 m.

2.5. Molecular modeling

Steric energies and rotational barriers determining the favored phosphate conformations were calculated using the molecular mechanics program Tinker (Tinker v. 3.9, 2001, Ponder, J.W., Washington University School of Medicine, USA) with the MM3 (2000) force field [35] implemented [36]. MM3 uses terms for van der Waals forces,

electrostatic dipole interactions, hydrogen bonding and special correction for anomeric effects, a pseudo-Morse potential for bond stretching, a fourth order potential for angle bending and a Fourier series for modeling torsional energy. Cross-terms for torsion–stretch, torsion–bend and bend–bend interactions are included. A dielectric constant of 4.0 appropriate for carbohydrate simulations was used in all calculations [37]. All structures were energy minimized until the root mean square (rms) gradient was less than 0.001 kcal/mol/Å using a limited memory quasi-Newton algorithm [38]. While the calculations of the 6-*O*-glucoside were fully relaxed, the helical calculations were restricted to relax only the exocyclic C-6 group and neighboring hydroxyl groups. A few phosphate-related parameters missing in the original MM3 force field were adapted from a study on phosphosphingolipids [39].

To investigate the influence of 6-*O*-phosphate substitution on double helical amylose structures a molecular builder for carbohydrates (POLYS) [40] was used to generate and optimize the amylosidic double helical fragments.

3. Results

3.1. Features of the methyl α-D-glucopyranoside 6-O-phosphate crystal structure

The atomic labeling of methyl-D-glucopyranoside 6-*O*-phosphate is shown in Fig. 1 along with the most important torsional angles. The orientations of the torsion angles are also referred to as *gauche–gauche* (GG), *gauche–trans* (GT) or *trans–gauche* (TG), depending on whether the values of angles are closest to −60°, 60° or 180°.

The crystals are comprised of methyl glucopyranoside 6-*O*-phosphate anions and K^+ cations, connected by anion–cation interactions and hydrogen bonds between the anions. Methylation of the anomeric center has successfully locked the glucose unit in α position. Fig. 1 displays an ORTEP plot [41] of the molecular structure. The phosphate group carries a single negative charge, as the compound is the mono-potassium salt. The oxygen O-7 is protonated, and the similarity of the other P–O bond distances (1.489(2) and 1.5013(2) Å) suggests a delocalization of the negative charge. The potassium ion is surrounded by six ligands in an octahedral arrangement (Fig. 2). The four oxygen atoms in an equatorial plane are bound to carbon (O-$1_{[x,y,z+1]}$...K, O-$2_{[x,y,z+1]}$...K, O-$3_{[x,y,z+1]}$...K, O-$4_{[x,y,z+1]}$...K) and have K–O distances ranging from 2.620(1) to 2.996(1) Å. The remaining coordinating oxygen atoms (bound to phosphorus), O-$7_{[x,y,z+1]}$...K and O-$8_{[x,y,z+1]}$...K, form angles of 89° and 68° with this plane, respectively. Since each phosphate group is involved in two different oxygen–potassium coordinations, one of them is 'bound' to distort the octahedral and the coordination around the K^+ is further

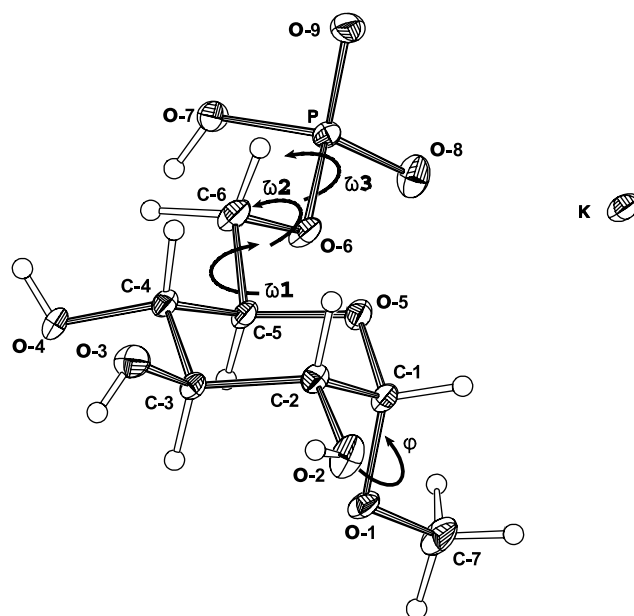Fig. 1. ORTEP drawing of methyl α-D-glucopyranoside 6-*O*-phosphate including thermal ellipsoids and atomic labeling. The orientation of the phosphate group is described by the following torsion angles: ωl = O-5–C-5–C-6–O-6, ω2 = C-5–C-6–O-6–P and ω3 = C-6–O-6–P–O-7(H). The orientation of the methyl substituent attached to the anomeric carbon is described by the torsional angle: ϕ = O-5–C-1–O-1–C-7.

distorted by significant interactions through O-$3_{[x,y,z+1]}$...K (3.370(1) Å) and O-$2_{[x,y,z+1]}$...K (3.086(1) Å). Four intermolecular O–H...O hydrogen bonds are found in the crystal which all involve the phosphate oxygen atoms that do not function as ligands to K^+: O-7–H...O-$9_{[x,y,z+1]}$ (1.75(2) Å), O-2–H...O-$9_{[x+1/2,-y+5/2,-z+1]}$ (2.41(2) Å), O-3–H...O-$8_{[x+1/2,-y+5/2,-z+2]}$ (1.84(2) Å) and O-4–H...O-$9_{[-x-1/2,-y+3,z+1/2]}$ (1.99(2) Å). None of the O–H oxygen atoms acts as acceptors, thus neither the ring O-5, the methyl O-1 nor the 6-*O*-phosphate ester accept a hydrogen bond. The low number of hydrogen bonds appears to be a consequence of a favored potassium coordination. The phosphate oxygen O-9, that is not involved in the coordination of the potassium ion, is acceptor of three hydrogen bonds, of which the one donated by phosphate oxygen O-$7_{[x,y,z+1]}$ is rather short (2.56 Å). A search for chemically equivalent hydrogen bonds in the Cambridge Structural Database (CSD, [42]) places this hydrogen bond length very close

Table 2
Conformational features related to the phosphate and the methoxy geometry

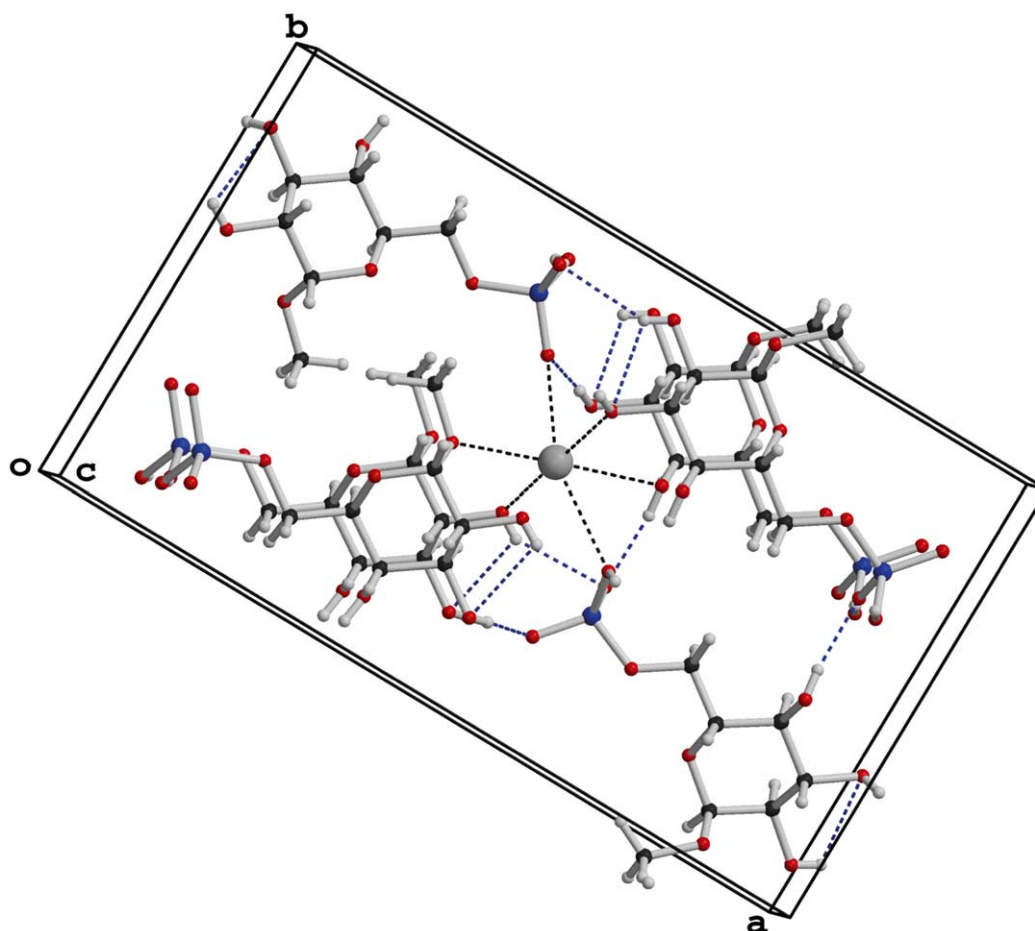|	Me α-Glc	(1)	(2) [43]	(3) [44]	(4) [45]	(5) [45]
Anomer	α	α	β	β	β	α
Ring	$^4C_1$	$^4C_1$	$^4C_1$	$^4C_1$	$^4C_1$	$^4C_1$
C-1–O-1		1.41	1.37	1.38	1.38	1.31
O-6–P	–	1.59	1.62	1.57	1.61	1.63
τ(C-6–O-6–P)	–	120.7	120.1	120.4	120.2	118.7
τ(O-6–P–O-7)	–	105.8	101.6	106.3	102.5	108.1
τ(O-6–P–O-8)	–	105.8	107.2	107.5	107.4	101.3
τ(O-6–P–O-9)	–	111.4	108.0	107.2	107.3	107.9
τ(O-8–P–O-9)	–	116.8	112.2	118.3	111.7	113.5
ωl		62.7	−68.2	63.8	57.7	60.5
ω2	–	−170.6	−119.6	−144.1	116.1	98.8
ω3	–	−68.4	169.2	65.2	171.2	59.7
ϕ		69.3	–	–	–	–

Comparison with similar glucose 6-*O*-phosphate structures.

Fig. 2. Octahedral coordination of the potassium ion. Unit cell axis and hydrogen bonds are also illustrated.

to the mean value for the P=O...H–O–P type (2.562 Å for 311 bonds).

3.2. Methyl α-D-glucopyranoside 6-O-phosphate conformation

Table 2 summarizes main conformational features of the methyl α-D-glucopyranoside 6-O-hydrogenphosphate and compares it to similar 6-O phosphorylated glycosides found in the literature. A search for the 6-O phosphorylated glucose ring fragment (CSD) resulted in four related structures: barium D-glucose 6-O-phosphate heptahydrate [43] (2), sodium D-glucose 6-O-(hydrogen phosphate) [44] (3), bis(cyclohexyl-ammonium) D-glucose 6-O-phosphate trihydrate [45] (4) and (5). All five structures possess the $^4C_1$ chair conformation of the hexopyranose ring and there is no evidence that the phosphate group significantly distorts the ring structure, as the pucker parameters display only little deviation from the ideal values.

Unlike the sulfate group which can only be deprotonated to the $R–O–SO_3^-$ form, the phosphate group can have different states of protonation as $R–O–PO_3H_2$, $R–O–PO_3H^-$ or $R–O–PO_3^{2-}$. Moreover, the phosphate group exhibits a significantly more variable geometry than the sulfate group (Table 2). As an example, the phosphate ester bond O-6–P varies from 1.57 to 1.63 Å, the O–P–O_P valence angle varies from 102 to 111° and the O_P–P–O_P valence angle varies from 101 to 118°. The structure of the phosphate group of the new 6-O-

phosphate glucoside falls within the range of previously studied phosphates, but the overall conformation of the phosphate group deviates from the previous studies on the glycopyranose 6-O-phosphates. The torsion angles $\omega1$ and $\omega2$ reveal the conformation about the exocyclic C-5–C-6 and O-6–P bonds, respectively, and thereby the orientation of the phosphate group (Fig. 1). The O-6 position defined by the $\omega1$ dihedral angle is found in a perfect staggered GT position found in all but one structure, namely, the barium heptahydrate (2). According to a study of 101 conformations of aldohexopyranoses found in crystal structures, this is the preferred conformation of the primary hydroxyl group (60%) [46]. The $\omega2$ dihedral angle defining the position of the phosphor atom is apparently more variable and our structure falls close to a staggered *anti* position in contrast to the other structures which are all more eclipsed. The orientation of $\omega3$ defining the hydrogen phosphate position is not considered important, as it is primarily used to optimize the hydrogen-bonding network in the crystal.

The methoxy group is found in the $\phi = 60$ conformation which is the favored conformation for glucosides, as it optimizes the exo-anomeric effect. This is naturally also the conformation which is present in double helical amylopectin [4,7] and thus emulates the amylopectin elongation.

To investigate the energetic aspects concerning the orientation of the phosphate group, a relaxed energy map of methyl
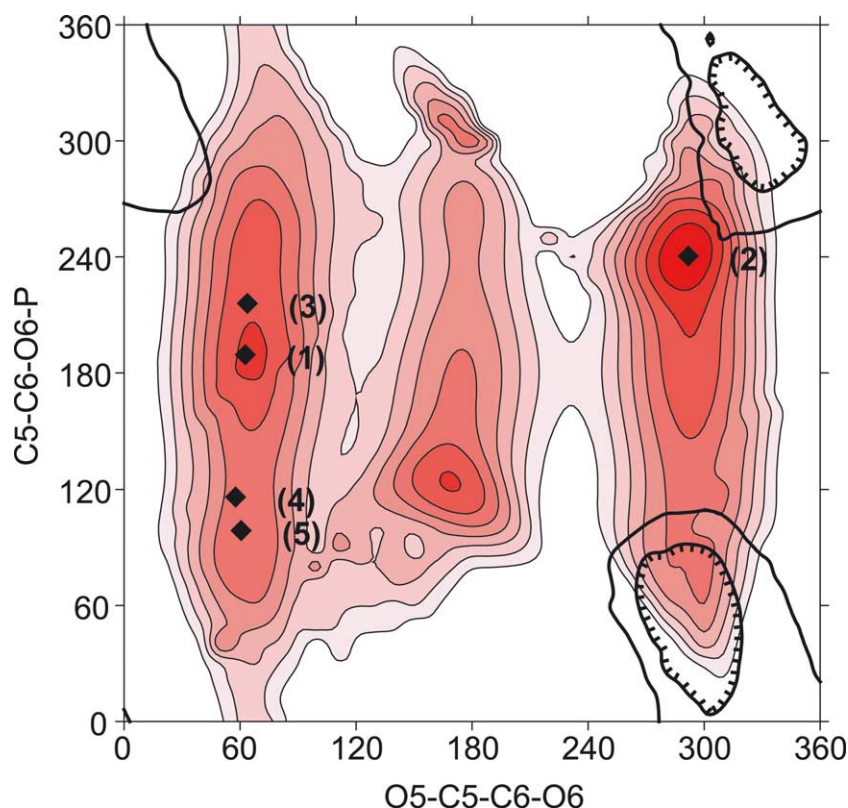
Fig. 3. Relaxed map of methyl α-D-glucopyranoside 6-O-phosphate as a function of the two torsional angles defining the 6-O-phosphate geometry. The map was calculated by driving ω1 and ω2 in 10° increments resulting in 36×36 mesh-points (structures) and keeping φ relaxed in the 60° position. Iso-contours are drawn from 0–8 kcal/mol. Positions of the phosphate geometries found in other 6-O-phosphate glucosides are superimposed. The bold iso-contour lines are the 10 kcal/mol steric barriers for the phosphate group when optimized in the double amylosidic structure.

α-D-glucopyranoside 6-O-phosphate was calculated, while keeping the methoxy group (relaxed) in the favored position predicted by the exo-anomeric effect and also found in the present crystal structure. In this study the methoxy group was added in order to prevent mutarotation and if possible to simulate the elongation of the α-glucan. The global energy minimum on this relaxed map (Fig. 3) is found at ω1 = 70° and ω2 = 180°, which is practically identical to the crystal conformation found in the potassium salt (1), implying that the structure was able to propagate in the crystal lattice in a
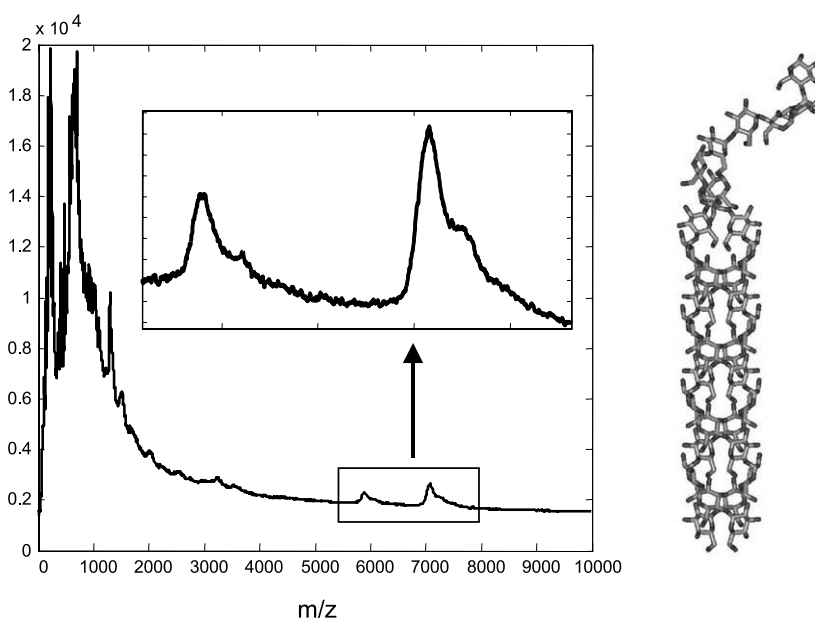

Fig. 4. MALDI-TOF mass spectrum of mildly fragmented potato starch. Peaks with higher molecular shoulders are centered at 5898 and 7078 Da (corresponding to 33 and 40 glucose units, respectively).

relaxed high probability conformation. However, as evident from the relaxed energy map, all the other crystal structures of phosphated glucosides are found in similar low energy regions, all within 1 kcal/mol from the global minimum. Especially the $\omega2$ appears to be rather flexible and allow the phosphate group to adjust according to local environment.

The double helical nature of A- and B-types of starch is well established from X-ray scattering experiments and molecular modeling [4,5], and recently complete atomic scale structures have been proposed for the double helical fragment [7]. For potato starch the peak degree of polymerization of the amylopectin side chains obtained after enzymic debranching is between DP 18 and DP 22 [15]. To this end, we have conducted some simple MALDI-TOF mass spectrometry experiments of gelatinized amylopectin isolated from potato starch. MALDI-TOF analysis of carbohydrates does not reach the quality and sensitivity as obtained for peptides [47]. However, we succeeded in identifying two fragment species with molecular weights of 5898 and 7078 g/mol corresponding to 33 and 40 glucose units, respectively, both having a secondary smaller peak (shoulder) corresponding to one additional glucose unit (Fig. 4). This result is in accordance with proposed dimensions of double helical amylopectin motifs in native granular starch [7]. The DP 33 and DP 34 motifs correspond to a double helical fragment with 26 glucose units in a perfect double helical structure and four glucose units forming the $\alpha(1-6)$ joint and three to four glucose units to form the link to the next double helical fragment, as suggested in the so-called $M,N = 1,3$ and $1,4$ structures [7]. Furthermore, these dimensions fit well with the proposed one-branch point containing crystalline (double helical) segments obtained after long-term acid hydrolysis of starch (Nägeli dextrins) [8,48]. In the same manner, the DP 40 and DP 41 fragments could correspond to a structure with a longer double helical or linking motif corresponding in size (DP 18–22) to the linear single-stranded fragments obtained after debranching. It also agrees well with the ~ 7 nm crystalline lamellar dimensions obtained by models obtained from SAXS data [3]. Hence, the break-points providing the fragments obtained in the MALDI-TOF experiments most likely reflect cleavage at weak, amorphous branch point regions of the amylopectin molecules.

While the amorphous region of amylopectin (starch) is less well defined, the double helical crystalline regions are well established. For this reason we investigated the possible phosphorylation site in the double helical amylopectin structure.
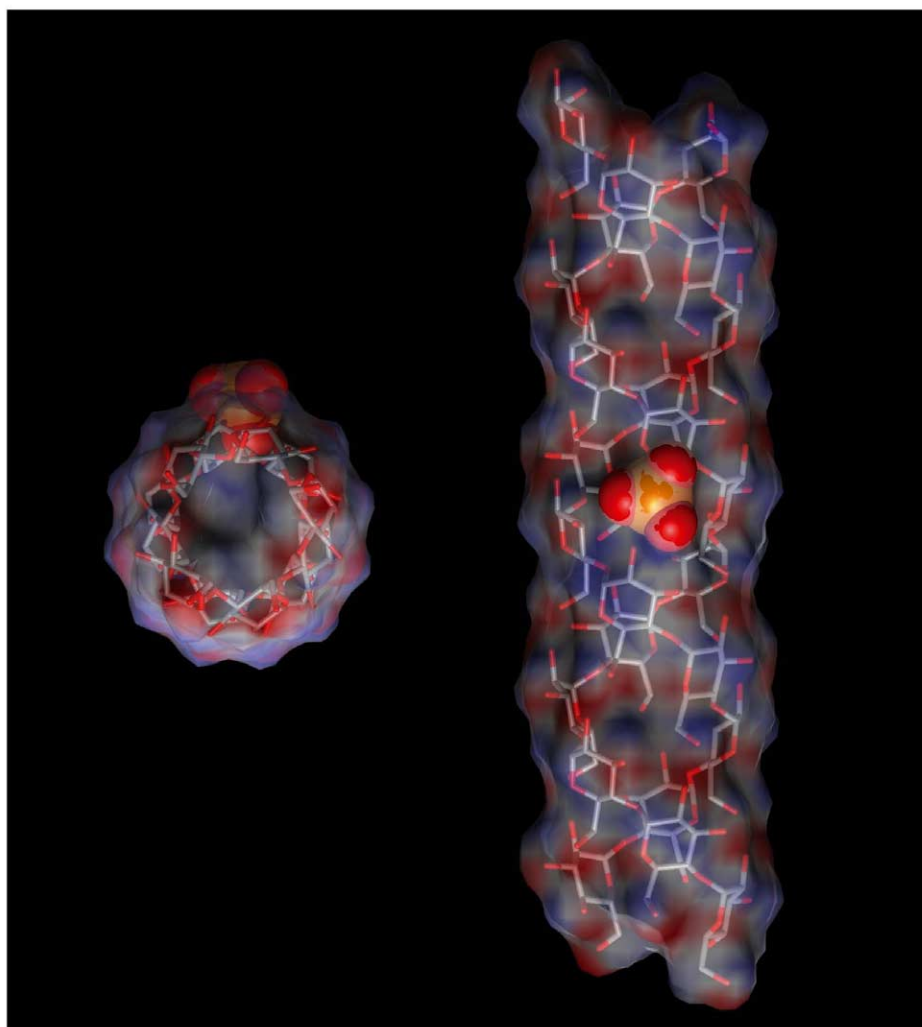

Fig. 5. The phosphate group added to the proposed double helical structure of amylopectin in the optimal position. Left: Top view. Right: Side view.

To this end we constructed a double helical amylopectin structure consisting of two 12 glucose unit single strands, according to the geometry proposed by O'Sullivan and Pérez [7]. One of the single strands was phosphorylated at the center glucose residue and subsequently rotated as a function of $\omega 1$ and $\omega 2$ and the conformational energy of the 'active' part of the entire structure minimized. The result is indicated in Fig. 3 by the solid bold line which gives the steric (≥ 10 kcal/mol) border over possible phosphate geometries of double amylopectin. Most interestingly, the possible phosphate geometries do not compare well with any of the existing 6-O-phosphate structures including (1). The global minimum was found at $\omega 1 = 290$ and $\omega 2 = 60$ which thus far has not been encountered in a crystal. This structure is shown in Fig. 5, which indicates that this particular phosphorylation site is well integrated into the double helical structure and does not appear to significantly affect the double helical diameter which, in turn, will allow starch phosphorylation without disrupting the hexagonal packing of the double helical amylopectin fragments.

4. Discussion

Despite the fact that the newly synthesized glucopyranoside 6-O-phosphate (1) only differed slightly from previously known glucoside 6-O-phosphate structures, this study contributes to the evidence that describes the phosphate geometry of a glucoside 6-O-phosphate as a flexible functional group that can adapt its conformation to the local steric and chemical environment. The geometry of the phosphate group in (1) was found to be practically identical to the one predicted as the global minimum structure by molecular mechanics procedures. This supports the use of such procedures in the extrapolation to double helical amylopectin fragments as well as explains the easy growth of crystals.

When the phosphate geometry of (1) was extrapolated to a double helical amylopectin fragment, it was found that it represented a sterically hindered site, as did all previously determined 6-O-phosphate structures. It is however possible that minor adjustments of the double helical structure will also allow for the phosphate geometry found in the heptahydrate barium salt of glucose 6-O-phosphate (2) to be encompassed in the crystalline domains of amylopectin, which in turn may suggest that the orientation of the 6-O-phosphate group is significantly influenced by the presence of water.

Most importantly, this study demonstrates that 6-O phosphorylation of double helical amylopectin fragments in the crystalline domains of starch is possible without significant perturbation of the hexagonal packing of amylopectin double helices in the starch granule. Keeping in mind the fact that one out of 100–200 glucose units in normal starches is phosphorylated, this result indicates that much higher degrees of phosphorylation in the double helical domains may be possible, providing that interaction with the counterions can be optimized.

Future studies should aim at investigating double helical interactions with and without phosphorylation, including counterion cross-bindings as well as investigating other possible phosphorylation sites such as the proposed 3-O phosphorylation, which we preliminarily have found to protrude from the double helical structure and thus to prevent optimal chain–chain interactions in the hexagonal amylopectin packing. This may certainly have implications for starch lamellar crystallinity, integrity and enzyme degradability and may help explaining the link between starch phosphorylation and starch degradation as observed in Arabidopsis and the potato plant models.

References

[1] Oostergetel, O.G.T. and Van Bruggen, E.F.J. (1993) Carbohydr. Polym. 21, 7–12.
[2] Waigh, T.A., Perry, P., Riekel, C., Gidley, M.J. and Donald, A.M. (1998) Macromolecules 31, 7980–7984.
[3] Jenkins, P.J., Cameron, R.E. and Donald, A.M. (1993) Starch/Stärke 45, 417–420.
[4] Imberty, A., Chanzy, H., Pérez, S., Buléon, A. and Tran, V.H. (1988) J. Mol. Biol. 201, 365–378.
[5] Imberty, A. and Pérez, S. (1988) Biopolymers 27, 1215–1221.
[6] Imberty, A., Buléon, A., Tran, V. and Pérez, S. (1991) Starch/Stärke 43, 375–384.
[7] O'Sullivan, A.C. and Pérez, S. (1999) Biopolymers 50, 381–390.
[8] Blennow, A., Bay-Smidt, A.M., Olsen, C.E. and Møller, B.L. (2000) Int. J. Biol. Macromol. 27, 211–218.
[9] Bay-Smidt, A.M., Wischmann, B., Olsen, C.E. and Nielsen, T.H. (1994) Starch/Stärke 46, 167–172.
[10] Schwall, G.P., Safford, R., Westcott, R.J., Jeffcoat, R., Tayal, A., Shi, Y.C., Gidley, M.J. and Jobling, S.A. (2000) Nat. Biotechnol. 18, 551–554.
[11] Blennow, A., Bay-Smidt, A.M., Wischmann, B., Olsen, C.E. and Møller, B.L. (1998) Carbohydr. Res. 307, 45–54.
[12] Tabata, S. and Hizukuri, S. (1971) Starch/Stärke 23, 267–272.
[13] Takeda, Y. and Hizukuri, S. (1982) Carbohydr. Res. 102, 321–327.
[14] Blennow, A., Bay-Smidt, A.M., Olsen, C.E. and Møller, B.L. (1998) J. Chromatogr. A A829, 385–391.
[15] Blennow, A., Engelsen, S.B., Munck, L. and Møller, B.L. (2000) Carbohydr. Polym. 41, 163–174.
[16] Veselovsky, I.A. (1940) Am. Potato J. 49, 330–339.
[17] Viksø-Nielsen, A., Blennow, A., Jorgensen, K., Kristensen, K.H., Jensen, A. and Møller, B.L. (2001) Biomacromolecules 2, 836–843.
[18] Wiesenborn, D.P., Orr, P.H., Casper, H.H. and Tacke, B.K. (1994) J. Food Sci. 59, 644–648.
[19] Smith, A.M. (1999) Curr. Opin. Plant Biol. 2, 223–229.
[20] Nielsen, T.H., Wischmann, B., Enevoldsen, K. and Møller, B.L. (1994) Plant Physiol. 105, 111–117.
[21] Lorberth, R., Ritte, G., Willmitzer, L. and Kossmann, J. (1998) Nat. Biotechnol. 16, 473–477.
[22] Ritte, G., Lloyd, J., Eckermann, N., Rottman, A., Kossmann, J. and Steup, M. (2002) Proc. Natl. Acad. Sci. USA 99, 7166–7171.
[23] Yu, T.S., Kofler, H., Hausler, R.E., Hille, D., Flugge, U.I., Zeeman, S.C., Smith, A.M., Kossmann, J., Lloyd, J., Ritte, G., Steup, M., Lue, W.L., Chen, J.C. and Weber, A. (2001) Plant Cell 13, 1907–1918.
[24] Blennow, A., Engelsen, S.B., Nielsen, T.H., Baunsgaard, L. and Mikkelsen, R. (2002) Trends Plant Sci. 7, 445–450.
[25] Lloyd, J.R., Landschutze, V. and Kossmann, J. (1999) Biochem. J. 338, 515–521.
[26] Abel, G.J.W., Springer, F., Willmitzer, L. and Kossmann, J. (1996) Plant J. 10, 981–991.
[27] Denyer, K., Clarke, B., Hylton, C., Tatge, H. and Smith, A.M. (1996) Plant J. 10, 1135–1143.
[28] Hanessian, S. and Lavallée, P. (1975) Can. J. Chem. 53, 2975–2977.
[29] Mouzin, G., Cousse, H., Rieu, J.-P. and Duflos, A. (1983) Synthesis 2, 117–119.
[30] Ichikawa, Y., Manaka, A. and Kuzuhara, H. (1985) Carbohydr. Res. 138, 55–64.

[31] Lipták, A., Jodál, I. and Nánási, P. (1975) Carbohydr. Res. 44, 1–11.
[32] Meldal, M., Christensen, M.K. and Bock, K. (1992) Carbohydr. Res. 235, 115–127.
[33] Blessing, R.H. (1987) Cryst. Rev. 1, 3–58.
[34] Sheldrick, G.M. (1986) SHELXS86, Program for the Solution of Crystal Structures.
[35] Allinger, N.L., Yuh, Y.H. and Lii, J.-H. (1989) J. Am. Chem. Soc. 111, 8551–8567.
[36] Allinger, N.L., Rahman, M. and Lii, J.-H. (1990) J. Am. Chem. Soc. 112, 8293–8307.
[37] French, A.D., Rowland, R.J. and Allinger, N.L. (1990) in: (French, A.D. and Brady, J.W., Eds.), Computer Modelling of Carbohydrate Molecules, pp. 120–140, American Chemical Society, Washington, DC.
[38] Ponder, J.W. and Richards, F.M. (1987) J. Comput. Chem. 8, 1016–1024.
[39] Dupré, D.B. and Yappert, M.C. (1999) J. Mol. Struct. (Theochem.) 467, 115–133.
[40] Engelsen, S.B., Cros, S., Mackie, W. and Pérez, S. (1996) Biopolymers 39, 417–433.
[41] Johnson, C.K. (1976) ORTEPII, Report ORNL-5138.
[42] Allen, F.H., Bellard, S., Brice, M.D., Cartwright, B.A., Doubleday, A., Higgs, H., Hummelink, T., Hummelinkpeters, B.G., Kennard, O., Motherwell, W.D.S., Rodgers, J.R. and Watson, D.G. (1979) Acta Crystallogr. Sect. B Struct. Sci. 35, 2331–2339.
[43] Lis, T. (1991) Acta Crystallogr. Sect. C Cryst. Struct. Commun. 47, 642–643.
[44] Viswamitra, M.A. and Narendra, N. (1985) Acta Crystallogr. Sect. C Cryst. Struct. Commun. 41, 1621.
[45] Lis, T. (1990) Acta Crystallogr. Sect. C Cryst. Struct. Commun. 46, 95–98.
[46] Marchessault, R.H. and Pérez, S. (1979) Biopolymers 18, 2369–2374.
[47] Mohr, M.D., Börnsen, K.O. and Widmer, H.M. (1995) Rapid Commun. Mass Spectrom. 9, 809–814.
[48] Jane, J.L., Wong, K.S. and McPherson, A.E. (1997) Carbohydr. Res. 300, 219–227.